Exploration of the Transition State for Tertiary Structure Formation between an RNA Helix and a Large Structured RNA

Supplementary Material

Laura E. Bartley, Xiaowei Zhuang, Rhiju Das, Steven Chu, and Daniel Herschlag

TABLE OF CONTENTS FOR THE SUPPLEMENTARY MATERIAL

OVERVIEW

We first present a supplementary Results section in which we compare our measurements with those made previously and describe observations relating to the short substrate, CUCU, that support the measured rate constant. Tables S1 and S2 enumerate Figure 4. ('S' preceding a number indicates that the table, reference, etc. are in the Supplementary Material, whereas, if no S is included the number refers to the published text.) Table S3 compares our temperature data to those determined previously. Next, we provide a further description of the materials used and a detailed description of our method of data analysis.

SUPPLEMENTARY RESULTS

Modifications to P1: Comparison with Previous Results. Compared with previous results at higher temperatures, different trends are observed in the effects on the equilibrium constant for docking (K_{dock}) of P1 duplex modifications measured here at 22 °C. A few modifications, including C(-1), d26, and d23, have effects that are within ~0.5 kcal mol^{-1} of those observed previously.[S1-S5] However, other positions gave different effects. The d(-2) and d(-3) modifications each destabilize docking by ~1.5 kcal mol^{-1} more than previously observed at 42 °C[S4] and 50 °C.[S2,S3] In contrast, d25 has a ~1.5 kcal mol^{-1} smaller effect.[S2-4] The opposite trends for the two strands of the P1 duplex might be due to a temperature-dependent change in the core structure[S6,S7] or the orientation of P1 with respect to the core. Notably, the d25 modification has an increased effect (by 1 kcal mol^{-1}) in the L-16 context relative to L-21; whereas, the m(-3) substrate modification has a smaller effect in L-16 than L-21. Although the details are not currently understood, together these results suggest that the

structures that stabilize the docked state may vary depending on the conditions or that different underlying molecular events give rise to different thermodynamic signatures.

Coupling with Guanosine. Guanosine increases the equilibrium for docking, K_{dock}, by ~3-fold. Within error, all of the effect is manifested in a slower rate constant for undocking. However, based on an indirect measurement, a previous study concluded that the rate of docking of an oliognucleotide product slows 3-fold due to binding of G.[S8] The K_d for product binding reported in that study is ~10-fold weaker than expected, based on extrapolation from higher temperatures of the difference in K_{dock} between oligonucleotide product and substrate.[S9,S10] This suggests that the previous study may have examined a misfolded form of the ribozyme.[S11] Indeed, the previous study[S8] reported 5-fold anti-coupling between oligonucleotide product and G; whereas, a ≤2-fold effect of G on the equilibrium for product binding is found with correctly folded ribozyme (K. Karbstein and D.H. unpublished results).

Docking for the Short Substrate. The short substrate (CUCU) gives a k_{dock} that is similar to k_{blink} (Scheme 1). However, the absence of undocked events that are longer than 300 ms (in >2200 seconds of observation time), strongly suggests that the rate constant for the short S is at least as great as reported and is not an artifact due to misidentification of photophysical events. Further, if all or most of the undocking events for the short S were due to blinking, than the number of low FRET events per observation time (frequency) would be expected to be similar to the frequency of blinking for ribozyme with full-length S or the DNA control. Instead, the frequency of low FRET events for the short S (0.22 events s^{-1}) is much higher than the frequency of blinking events for wt (L-21) and the L-16 ribozymes (0.02 and 0.06 events s^{-1}, respectively), as well as the DNA control (0.01 events s^{-1}). In

addition, fits of the data from the short S with the first one and two bins (18 and 36 ms) excluded, which contain most blinking events ($\tau_{blink} \approx 20$ ms), give the same rate constant for docking ($k_{dock} = 40 \pm 7$ and 37 ± 6 s^{-1}, respectively) as when all the data are fit ($k_{dock} = 35 \pm 5$ s^{-1}).

Table S1: Effect of urea on the kinetics and thermodynamics of P1 docking.[a]

urea (M)	K_{dock}[b]	k_{dock} (s^{-1})	k_{undock} (s^{-1})	$ß^{‡}$[c]
0	32 ± 4[d]	3.3[e] ± 0.4	0.15[g] ± 0.02	-
1	13 ± 3	2.8[e] ± 0.6	0.28[g] ± 0.07	-
2	4.4 ± 0.5	3.0 ± 0.2	0.61[h] ± 0.07	-
2.5	2.3 ± 0.3	2.9 ± 0.3	1.1[i] ± 0.1	-
3	1.6 ± 0.1	2.5[f] ± 0.1	1.4[i] ± 0.1	-
4	0.56 ± 0.05	2.1[f] ± 0.1	2.9[i] ± 0.2	-
5	0.11 ± 0.03	1.8[f] ± 0.4	6[i] ± 1	-
m (kcal mol^{-1} M^{-1})[j]	0.65 ± 0.05	0.07 ± 0.04	-0.44 ± 0.05	0.1 ± 0.1

[a] Measured at 22 °C, 10 mM $MgCl_2$, pH 7.0, for the L-16 ribozyme for which the IGS is extended by five residues relative to the L-21 ribozyme. Measurement were made on four different days. Dupliate conditions were analyzed together.

[b] K_{dock} calculated from the total time spent in the docked state over total time spent in the undocked state.

[c] The ratio of $m^{‡}(k_{dock})/m(K_{dock})$ indicating the fractional change in accessible surface area in the transition state relative to the docked state.

[d] Errors are two times the standard deviation based on Poisson statistics and are calculated as $1/\sqrt{N}$, where N is the number of events observed under a given set of conditions.

[e] $k_{dock}^{(2)}$, the rate constant for the second phase of the undocked time histogram, which excludes photophysical events.

[f] k_{dock}, corrected for undercounting of short undocked events.

[g] $k_{undock} = k_{undock,obs}^{(2)} - k_{photobleach} - 1/(\text{trace length})$.

[h] $k_{undock} = k_{undock} - k_{photobleach} - 1/(\text{trace length})$.

[i] k_{undock}, corrected for undercounting of short docked events.

[j] The relatively large errors in m-values and imperfect agreement between the m-values determined from the rate versus the equilibrium data arise largely from limitations in the data at 0 and 5 M urea. At 0 M urea there is considerable error in k_{undock} due to the small number of events used and other biases (see Supplementary Materials and Methods), and at 5 M urea the data are consistent with the presence of two ribozyme populations with different rate and equilibrium behavior. Omission of these points gives improved agreement but does not significantly change the m-values, nor does it effect the conclusions drawn.

Table S2. Effects of Temperature on the Kinetics and Thermodynamics of m(-3) Docking [a]

Temperature[b,c] (°C)	K_{dock}[d]	k_{dock}[e] (s^{-1})	k_{undock}[f] (s^{-1})
10	0.25 ± 0.08[g]	1.1 ± 0.2	3.5 ± 0.6
12	0.32 ± 0.07	0.9 ± 0.2	4.0 ± 0.8
14	0.40 ± 0.03	2.0 ± 0.1	5.1 ± 0.3
17	0.6 ± 0.2	2.0 ± 0.5	3.6 ± 0.9
17	0.31 ± 0.09	1.9 ± 0.4	5.7 ± 1.0
19	0.7 ± 0.1	3.0 ± 0.4	4.8 ± 1.0
22	0.42 ± 0.07	2.7 ± 0.4	8 ± 1
23	0.50 ± 0.06	3.3 ± 0.3	7.4 ± 0.7
27	0.45 ± 0.09	4.8 ± 0.8	13 ± 2
33	0.55 ± 0.09	7 ± 1	15 ± 2
33	0.70 ± 0.06	6.6 ± 0.5	12 ± 1
38	1.1 ± 0.1	13 ± 1	13 ± 1
43	1.3 ± 0.3	13 ± 2	9 ± 1

[a] Measured at 10 mM $MgCl_2$, pH 7.0 (at 22 °C), for the L-16 ribozyme for which the IGS is extended by five residues relative to the L-21 ribozyme.

[b] Calculated temperature of the slide based on a four point calibration of the difference between air temperature and the temperature of the water pumped around the sample cell and objective. Errors are estimated as ±1 °C at the temperature extremes down to ±0.5 °C at 22 °C.

[c] Measurements were made on three different days with different temperature series, including duplicate temperatures, as shown.

[d] K_{dock} calculated from the total time spent in the docked state over total time spent in the undocked state.

[e] k_{dock}, corrected for undercounting of short docked events. This adjustment had no effect within error in most cases.

[f] k_{undock}, corrected for undercounting of short undocked events.

[g] Errors are two times the standard deviation based on Poisson statistics and are calculated as $1/\sqrt{N}$, where N is the number of events observed under a given set of conditions.

Table S3. Summary of Thermodynamic and Activation Parameters for Docking Measured in This and Previous Studies.

P1	Ref.	T (°C)	ΔH (kcal mol^{-1})	$\Delta H^{\ddagger}$ (kcal mol^{-1})	ΔS (e.u.)[b]	$\Delta S^{\ddagger a}$ (e.u.)[b]
m(-3)[c]	this study	10 - 43	8 ± 2		25 ± 6	
CCCUCUA[d]	S12	30 - 50	19 ± 9		62 ± 30	
m(-3)[c]	this study	10 - 43	-	12 ± 2		-14 ± 4
$CUCUA_5$[d]	S9	30 – 60	-	5 ± 10		-37 ± 27
pyrCUCU[d,e]	S13	10 - 25	-	22		21

[a] Calculated with the pre-exponential factor measured for chemical reactions (see footnote †).
[b] e.u. = entropy units = cal mol^{-1} K^{-1}
[c] L-16 ribozyme, with the fully base-paired, extended P1 duplex. m(-3) indicates that the 2′-hydroxyl at the –3 position was replaced with a 2′-methoxy (see Fig 1*c*).
[d] L-21 ribozyme.
[e] 'pyr' indicates the position of a pyrene fluorophore.

SUPPLEMENTARY MATERIALS AND METHODS

Oligonucleotide Preparation. Oligonucleotide substrates contained 3′-three carbon, amino modifications for attachment of dyes. Substrates were deprotected during a 30 min incubation in 200 mM sodium acetate, pH 3.3 at 60 °C,[S14] followed by addition of sodium carbonate (final: 150 mM, pH 8.5) and a 5-fold excess of Cy3 or Cy5 NHS-ester (Amersham-Pharmacia). Labeling reactions were carried out at 37 °C for 12 hours, followed by ethanol precipitation to remove excess dye. Oligonucleotides were then purified via anion exchange high pressure liquid chromatography.[S15,S16] 5′-Biotinylated, 3′-amino modified, deoxyribo-oligonucleotide tether was purchased from Dharmacon, Inc. and dye-labeled as above. Oligonucleotides for ligation reactions were purchased from Dharmacon or the Stanford University Protein and Nucleic Acids Facility, deprotected according to the manufacturers' protocols, and purified on 8 M urea/15% acrylamide gels.

Ribozyme Ligations. Modified ribozymes were created by ligation of the appropriate synthetic oligonucleotide (modifying oligo) to a transcribed L-38,T ribozyme. Minor modifications to previous protocols[S17,S4] to increase ligation efficiency and prevent cleavage of the 3′-extention used to immobilize ribozyme to the surface were developed. Ribozyme, oligonucleotide splint, modifying oligo, and an oligonucleotide complementary to the last 44 residues of the ribozyme including the 3′-extension (anti-3′oligo) were annealed in 200 mM NaCl, 25 mM sodium MES (2-morpholinoethanesulfonic acid), pH 5.5 by heating for 3 minutes at 95 °C followed by cooling for ≥10 minutes at room temperature. Final ligation reaction conditions were 22 °C, 50 mM sodium EPPS [*N*-2-(hydroxyethyl)piperazine-*N*-3-propanesulfonic acid], pH 7.5, 4 mM $MgCl_2$, 1 mM ATP (adenosine triphosphate), 50 mM

NaCl, 100 mM DTT (dithiothreitol), 1 μM ribozyme, 3 μM modifying oligo, 3 μM anti-3´oligo, 2 μM splint, 1 μM his-tagged T4 DNA ligase for 12 hours. Reactions were stopped with EDTA, ethanol precipitated, and ribozymes were purified on 8M urea/4% acrylamide gels.

Single-molecule Measurements. The general method for taking single-molecule fluorescence docking measurements was as described previously,[S16] although several improvements in data analysis have been instituted. As described below, these improvements include a method for quantitative, semi-automated analysis of single-molecule docking data and corrections for systematic biases in the data. Except for the attribution of the fast phase in the undocked time histogram to photophysics, the corrections for biases do not qualitatively affect the interpretations of the data but do increase the accuracy of the reported rate constants.

Sample Cell Preparation. Cells for single-molecule measurements were prepared from two glass coverslips, cleaned by flaming, and sandwiched together by double-sided sticky tape to form a 6 – 10 μL cell.[S16] Cells were incubated with 1 mg/mL biotinylated bovine serum albumin (Molecular Probes), rinsed, and incubated with 0.25 mg/mL streptavidin (Moelcular Probes) followed by a final rinse with 10 mM $MgCl_2$, 50 mM sodium MOPS pH 7.0. Immediately before use, background fluorescence measurements were taken on each slide.

Sample Preparation. 3′-Extended ribozymes (1 μM) were annealed to 5′-biotinylated, 3′-Cy5 labeled DNA oligonucleotide complementary to the 3′-extension (DNA tether, 250 nM) at high salt (500 mM NaCl, 50 mM sodium MES, pH 5.3; 95 °C for 30 s, cooled to 37 °C at 0.1 °C s^{-1}), followed by folding at 50 °C in 10 mM $MgCl_2$ at pH 5.3 for 30 minutes. Ribozymes were then placed on ice until measurements were taken. Ribozyme (100 nM) and substrate (200 nM) were mixed and diluted to ~100 pM before addition in 100 μL to streptavin-coated cells.

Experimental Apparatus. Single-molecule measurements were taken with a scanning confocal microscope as described previously[S18,S16,S19] with limited modifications. Excitation of donor dye at 514 nm was provided by an argon laser (Coherent Inc., Santa Clara, CA). A band pass filter (675/50) was placed before the detector for the acceptor.

Data Collection. For a typical experiment, a 14 μm by 14 μm region of a sample cell was scanned and single molecules located. The positions of molecules were manually identified based on the fluorescence signal in the acceptor channel. Selection of molecules from the donor channel yielded a large fraction (~0.5) of molecules that gave only a donor signal primarily due to damaged acceptor dyes. After identifying molecules, data were collected for a fixed amount of time at each position specified. After all identified molecules were examined, the process was usually repeated on one or more other regions of the sample cell. Acceptor and donor fluorescence intensity signals were collected in 3 or 5 msec bins.

Time Trace Analysis. Donor and acceptor fluorescence intensity time trace data were analyzed with the method briefly outlined here and described below. Manipulation of data and assignment of docked and undocked events was carried out with in-house programs written for Matlab (The MathWorks, Inc.). Data were corrected for background fluorescence and leakage of donor signal into the acceptor channel. Data were then combined into coarser time bins so that a change in signal representing a docking event could be distinguished from noise. Next, each time bin was assigned to the docked or undocked states based on FRET signal and total fluorescence signal (Fig 2). The equilibrium constant for docking was calculated from the total time spent in the docked state divided by the total time spent in the undocked state [$K_{dock,total}$ = (time docked)/(time undocked)]. From the assignment of each time bin to the docked or undocked states, the time spent in one state before transitioning to the next, termed dwell time, was calculated. The cumulative number of events at each dwell time in the docked and undocked states were plotted and fit to obtain the rate constants for undocking and docking, respectively (Fig 3).

Corrections to the rate constants for systematic bias in the data increased the agreement between $K_{dock,total}$ and the equilibrium constant for docking calculated as the ratio of rate constants ($K_{dock,kinetic} = k_{dock}/k_{undock}$). Depending on the time constant for undocking, different corrections were made to the docking and undocking rate constants to account for systematic errors in the data. When undocking was slow, short photophysical 'blinking' events occurred frequently relative to undocking events (Scheme S1). A fraction of blinking events is misidentified as undocking due to noise in the data, leading to the requirement to fit the undocked and docked times by two exponentials. The slower exponential was attributed to P1 docking, and the faster exponential to blinking. Also when undocking was slow, the

observed rate constant for undocking was overestimated due to a bias toward observation of short docked events. This bias arose from short trace time due to photobleaching and data collection time relative to the observed time constant for undocking. When undocking was fast, the observed rate constants for docking and undocking were corrected for bias due to undercounting of events caused by a long bin time relative to dwell times for undocking.

Background Correction. Prior to assignment of docked and undocked events, the fluorescence signals from each channel were corrected for background fluorescence. The measured background fluorescence of a slide with no ribozyme added was <5% of the fluorescence signal from a ribozyme. The leakage of donor fluorescence into the acceptor channel allowed by the filter set used was determined to be 0.11 of the donor signal.

Binning. Fluorescence data taken in 3 or 5 ms bins were generally combined into 18 or 20 ms bins. Achievement of good signal-to-noise was first judged visually by clearly distinguishable docked and undocked fluorescence states (Fig 2). Time traces that required longer bins were not included in the final analysis. Although when the docked state was long-lived relative to the bin sixe [$\tau \approx 5$x(bin size)], fits of these data gave the same rate constants within error as the more finely binned data. A few exceptions were made to the use of 18-20 ms averaging. Good signal-to-noise required ~40 ms binning for d(–1) with and without guanosine and wt at 100 mM $MgCl_2$, which have higher than average equilibria for docking. For these situations, reducing the laser intensity for data collection decreased the rate constant for photobleaching and thus increased the number of complete docking events observed (see Corrections for Time Trace Truncations, below); this then required coarser binning. In

contrast, m25 has a very low equilibrium constant for docking (see Results) resulting in many docked events with durations (dwell times) shorter than 18 ms. The laser intensity at which these data were collected was sufficient to give good signal-to-noise with 9 ms binning, allowing the identification of significantly more docked events and a more accurate determination of the rate constants for docking and undocking.

Integral Plots. The lengths of time spent in the undocked state, or undocking 'dwell times,' were used to determine the rate constant for docking. Likewise, dwell times for docking indicated the rate constant for undocking. Dwell times were compiled from many molecules (see Reproducibility, below). First a histogram was constructed of the number of observed events with each dwell time with the binning resolution at which the data were analyzed. Next, the cumulative number of events observed with a dwell time less than or equal to each time increment were tallied and plotted versus time (Fig 3). Such a plot of the cumulative number of events is the equivalent of a plot of the integral of a histogram of dwell times; histograms are typically used to represent single-molecule dwell time data. Such 'integral plots' are useful for judging whether the dwell times are well described by one or more rate constants. In addition, relative to histograms, integral plots increase the weight of rare long events so that both long and short events can be fit appropriately by conventional least squares fitting algorithms such as the one used here by Kaleidagraph (Synergy Software). However, because the number of events are cumulative with respect to time, the errors associated with the fits of the integral plots underestimate the uncertainty associated with the data. Errors were therefore estimated independently of the fits as described below (in Error Estimates).

Integral plots were fit with a single exponential equation with an amplitude equal to the number of events observed, N (Eq S1). Dividing by N normalizes the scale to an

$$N(t) = N[1 - \exp(-k\,t)] \qquad [S1]$$

amplitude of 1, which allows data sets with different numbers of events to be compared, as shown in panels *b* and *c* of Figure 3. When distributions deviated systematically from single exponential behavior, the sum of two exponentials was used to fit integral plots with two rate constants (Eq S2). When double exponential fits are applied, the fastest rate constant is

$$N(t) = N[1 - A^{(1)}\exp(-k^{(1)}t) - A^{(2)}\exp(-k^{(2)}t)] \qquad [S2]$$

referred to as $k^{(1)}$, and its amplitude, as $A^{(1)}$.

Development of Criteria to Identify Docking and Undocking Events. Primary assignment of each time bin to the docked or undocked state was made on the basis of FRET efficiency (abbreviated FRET), where FRET efficiency = $[I_A/(I_A+I_D)]$ and I_A and I_D indicate the acceptor and donor signals after background correction. The average FRET of molecules that are predominantly in the docked and undocked states was found to be 0.9 ± 0.1 and 0.3 ± 0.2, respectively.[S16] From these values and a visual examination of assignment of docked and undocked events, thresholds for the docked state and undocked states were developed. Docked states were identified by FRET of >0.75; and undocked states were identified by a FRET of <0.5. Only molecules whose docked and undocked states generally conformed to these criteria were used. For most data sets, >80% of molecules were described well by these criteria.

Using the FRET criteria alone (without use of secondary screening criteria = unscreened),[§] a short-lived, low FRET state was observed in the ribozyme docking data that we attribute to a photophysical event (or class of events) associated with one or both of the dyes going to a dark state (Scheme S1). These short-lived, low FRET events, which we refer to as 'blinking' events, occur frequently in the data for the wt (L-21) ribozyme (*e.g.*, Fig 2a) and result in a significant fast phase in the plots of undocked times identified by FRET ($A^{(1)}$(unscreened) ≈ 0.7; $k_{dock}^{(1)}$ (unscreened) = $k_{unblink}$ ≈ 50 s^{-1}; at 4.8 W m^{-2}). Such blinking events are also observed in the unscreened undocking data for modified ribozymes (*e.g.*, m(-1); $A^{(1)}$(unscreened) ≈ 0.15; $k_{dock}^{(1)}$ (unscreened) = $k_{unblink}$ ≈ 45 s^{-1}; at 4.8 W m^{-2}). The fraction of blinking events decreases as modifications or other perturbations decrease the time spent in the docked state; that is, as K_{dock} decreases, $A^{(1)}$(fraction blinking) decreases, roughly (data not shown). This observation shall be discussed further below.

Scheme S1.

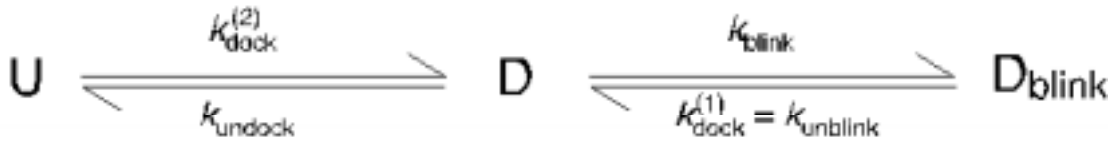

Three observations lead us to attribute the short-lived, low FRET events to photophysics. First, the fraction of short-lived, low FRET events observed in the unscreened undocked time data appears to increase with increasing laser power (Fig S1 triangles; R = 0.96; $p < 0.03$). This observation suggests that the short-lived events are induced by light, which is not expected for a ribozyme-associated event. Second, the FRET criteria for docking

[§] 'Unscreened' refers to data that have been evaluated for docking and undocking events with FRET criteria alone. 'Screened' refers to data that have been evaluated with FRET criteria as well as secondary screening criteria, as described in the section "Development of Criteria to Identify Docking and Undocking Events."

were used to analyze single-molecule time traces of a DNA duplex with a Cy3-Cy5 pair (40 base pairs with a 40 residue 3′-overhang, dyes at the duplex/single-strand junction). Even though the duplex molecule is not expected to undergo frequent conformational changes that give FRET changes, the analysis identified a short-lived low FRET state ($k_{unblink} \approx 65\ s^{-1}$; data not shown). This suggests that blinking is not dependent on the ribozyme, but may be a property of the dye pair employed. Third, a quantitative characterization of the short-lived, low FRET events for the ribozyme and the DNA control, found that most of these events result in a loss of fluorescence of one or both of the dyes (data not shown). In contrast, longer-lived, ribozyme-associated, low FRET events typically have the same total fluorescence signal as the average fluorescence for the entire trace [($\langle I_A+I_D \rangle$ per event) /($\langle I_A+I_D \rangle$ per trace) = 1.0 ± 0.13 for the wt ribozyme, where the notation, $\langle I \rangle$, indicates the average fluorescence intensity]. Different fluorescence properties of the two types of low FRET events are further evidence that the blinking events are different from the undocking events.

Together, this analysis suggests that blinking events are the result of laser-induced, short-lived dark states ($I \approx 0$) of one of the two dyes. Blinking of the donor dye results in a loss of fluorescence of both dyes, as in the events that are indicated with double-headed arrows in Figure 2*a*. Blinking of the acceptor dye results, in principle, in a FRET of ~0 and, with sufficient signal-to-noise, should be distinguishable from undocking events with a FRET of ~0.3. As discussed in the next section, blinking events cannot always be clearly distinguished from undocking events. We do not know the physical cause for blinking at this time. The dark state events described here appear to be longer lived ($\tau \approx 20$ ms) than what has been suggested to be a non-emitting triplet state described in another system with the same dye pair ($\tau \approx 0.2$ ms).[S20] Generally, the photophysical properties of the dyes in the group I

ribozyme system used here are complex. In addition to the 20 ms lifetime events, long-lived 'blinking' events ($\tau \approx 2$ s) occur with a frequency that is also dependent on laser power. Under typical conditions (~ 6 W m^{-2}) the frequency of such events was ~0.1 min^{-1}. These long blinking events were easily excluded manually from the data analysis and are not further discussed.

To develop criteria to exclude blinking events from our analysis, we used histograms that compared the fluorescence attributes of long-lived low FRET events (undocking) and the short-lived low FRET events (blinking events) (data not shown). A low FRET event in the *i*th time bin was considered to be an undocking event if it passed all of the following secondary screening criteria:

$$(I_{A,i} + I_{D,i}) > 0.61 \times (< I_A + I_D > \text{ per trace});$$

$$(I_{A,i}, I_{A,i-1}, I_{A,i+1}) > 0.1 \times (< I_A + I_D > \text{ per trace});$$

$$(I_{D,i}) > 0.2 \times (< I_A + I_D > \text{ per trace}).$$

Assignment of an undocked event due to infrequent (<1 per trace on average), unexplained transient increases in total fluorescence were excluded with the criterion:

$$(I_{A,i} + I_{D,i}) > 1.8 \times (< I_A + I_D > \text{ per trace}).$$

Events that pass these criteria are referred to as screened. However, as the distributions of short and long low FRET events overlapped, it was not possible to eliminate all misidentification of blinking events as undocking events.

The Fast Phases of Docking and Undocking Are Attributed to Blinking. After screening[§] by the FRET and fluorescence criteria described above, there is a smaller but still significant fraction of undocked events with shorter dwell times than expected from a single

exponential distribution (Figs 3*a*, 3*b*, and S1). Several lines of evidence suggest that the fast phase remaining after secondary screening is also due to photophysics (Scheme S1). First, even with screening, the number of and rate constant associated with the short undocked events observed with the wt ribozyme and the DNA duplex control data are similar in the same total time of observation (Fig 3*a*; N = 10 [DNA], $A^{(1)} = 8$ [ribozyme]; $k = 30 \pm 10$ s^{-1} [DNA], $k^{(1)} = 60 \pm 20$ s^{-1} [ribozyme]). This suggests that the fast phase is not related to the ribozyme but that it consists of blinking events that are indistinguishable from undocking events possibly due to noise in the raw data. Second, increasing laser power roughly correlates with an increasing fraction of undocked events in the fast phase (Fig S1 squares; R = 0.72; $p < 0.1$). As this analysis is confounded by the interdependence of the magnitudes of the rate constants and amplitudes of both phases, the rough agreement may be the best that can be expected. In contrast, if the fast phase were due to a ribozyme-related event, then the number of events observed should be independent of voltage. Third, a fast phase is observed in undocked time plots when substitutions cause K_{dock} to be above ~5. Perturbations, including urea and salt that decrease K_{dock} below this value also abolish the fast docking phase. If the fast docking phase were related to a different state(s) of the undocked ribozyme, all perturbations that decrease K_{dock} might not be expected to affect the alternative undocked state(s) in the same way. Instead, the disappearance of the fast phase with reduced K_{dock} is likely due to the reduction in the number of blinking events that occur from the docked state. (Blinking that occurs from the undocked state can also lead to a reduction in FRET and total fluorescence, but such events are not detected as a change in the ribozyme state, as the FRET is already low.) Finally, previous measurements of the rate constant for docking, though made under different conditions, did not identify a fast phase.[S21,S22,S13,S9]

For cases in which the time spent in the undocked state was better fit by the sum of two exponentials, the time spent in the docked state was often also better described by a double exponential (*e.g.*, Fig 3*c*; $A^{(1)} = 0.21$, $k_{undock}^{(1)} = 0.7 \pm 0.2\ s^{-1}$; $A^{(2)} = 0.79$, $k_{undock}^{(2)} = 0.15 \pm 0.01\ s^{-1}$). Two undocking rates are not predicted from simple models such as the one presented in Scheme S1, for which the observed rate constant for undocking, $k_{undock,obs}$, should be the sum of k_{undock} and k_{blink}. The occurrence of two phases of docked time plots only when blinking is observed in the undocked time plots, suggests that blinking may cause the two phases. In addition, the observation of two phases in the plot of the unscreened[§] high FRET dwell times for the DNA duplex control (data not shown, $A^{(1)} = 0.53$, $k_{blink}^{(1)}$ (unscreened) = 2.3 s^{-1}; $A^{(2)} = 0.47$, $k_{blink}^{(2)}$ (unscreened) = 0.55 s^{-1}) provides further evidence that the two phases in docked time plots are related to photophysics. Two apparent undocking rates may be caused by blinking at different rates from different dye states/orientations. Alternatively, molecules with lower than average fluorescence intensities may result in a disproportionately high misidentification of blinking events. Because blinking would be expected to artificially truncate docking events, we attribute the larger apparent undocking rate constant to the influence of blinking and the slower rate constant to undocking. For cases with two undocking phases, the choice of $k_{undock} = k_{undock}^{(2)}$ increases the agreement of K_{dock} calculated from the ratio of rate constants with K_{dock} calculated from total time spent in each state (see below in Calculation of K_{dock}). Because k_{blink}(screened)[§] $\approx 0.01\ s^{-1}$ is small relative to all k_{undock} (and $k_{undock}^{(2)}$) values reported, k_{undock} is not further adjusted to account for blinking.

Corrections for Time Trace Truncations. If the time constant for a process approaches the length of time that an observation is made then the measured rate constant will

be influenced by the time of observation. This bias is due to longer events being truncated by the ends of the trace so that only short complete events are likely to be observed. Thus, when K_{dock} is high, k_{undock} is biased due to truncation of traces due predominantly to photobleaching and to a lesser extent from data collection time per molecule. The effect of photobleaching on the observed rate constant for undocking was derived using Scheme S2. The correction for photobleaching on the observed rate constant for undocking is given by: $k_{undock,obs} = k_{undock} + k_{photobleach}$. Photobleaching from the undocked state can be neglected as the rate constant for photobleaching is much smaller than the rate constant for docking ($k_{photobleach} << k_{dock}$). The rate constant for photobleaching was determined by fitting the integrals of histograms constructed from traces that ended by photobleaching for each experimental condition (plots similar to Fig 3, with time of photobleaching on the x-axis). Independent of the modification examined, $k_{photobleach}$ increased with laser intensity, with a slope of 0.01 s^{-1} W^{-1} m^2 and a y-intercept of 0.0 (data not shown, R = 0.78, p < 0.01).

Scheme S2.

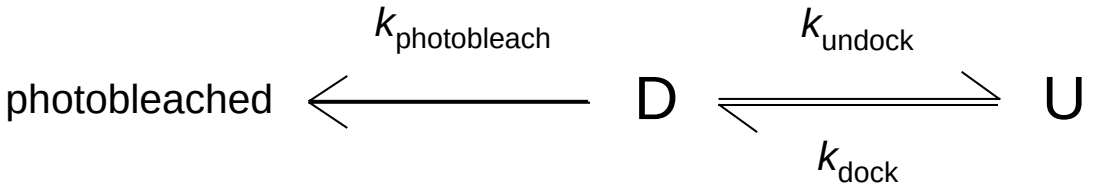

To optimize the amount of data collected, most data sets were collected under conditions in which the time of observation of each molecule (T) was chosen to be similar to the time constant of photobleaching. In a few instances the trace time (T) utilized is similar to the observed rate constant for undocking, so that the observed rate constant for docking is biased by the time of observation. The magnitude of the bias of $k_{undock,obs}$ due to trace time

was derived in the following manner. The probability of observing a complete event of duration t, when observation is made for time T is given by $P(t) = (1 - \frac{t}{T})$.

When $\tau < \sim 0.5*T$, the Taylor expansion of e^{-x}, ($e^{-x} = 1 - x + \frac{x^2}{2!} - \frac{x^3}{3!} + ...$) can be used to approximate $P(t)$; that is, $(1 - \frac{t}{T}) \approx \exp(-\frac{t}{T})$.

Equation 3S corrects for both trace time and photobleaching effects on the observed rate constant, and is derived from the following relationship:

$$\exp(-k_{\text{undock,obs}}t) = \exp(-k_{\text{undock}}t) \times \exp(-k_{\text{photobleach}}t) \times \exp(-\frac{t}{T}).$$

$$k_{\text{undock}} = k_{\text{undock,obs}} - k_{\text{photobleach}} - \frac{1}{T} \qquad [S3]$$

When the corrections due to photobleaching and trace time are ≥10% of the observed rate constant for undocking, the reported k_{undock} is calculated using Equation S3, as is noted in the legends of Tables 1A and 1B, S1, and S2. This corresponds to $k_{\text{undock,obs}}$ (or $k^{(2)}_{\text{undock,obs}}$) of <1 s^{-1}. In all cases, corrections due to trace truncation reduced the reported rate constants by ≤2-fold relative to the uncorrected values.

Undercounting of Short Events. Plots of the docked state dwell times for modifications with fast rate constants for undocking (>2 s^{-1}) contain fewer short (<40 ms) docked events than expected from a single exponential distribution (Fig 3*c*). Generally, undercounting of events is expected to occur when the dwell time of an event approaches the bin time. Limited signal-to-noise causes events that take place within a few bins (one or two) to fail to meet the FRET threshold for a docked event. To help reduce this effect, measurements of fast rate constants were examined with increased laser power. Additionally,

even with good signal-to-noise, photons that report on an event that has approximately the same duration as a bin may be split between two bins so that the signal is dampened and neither bin meets the criteria for docking. The number of events missed was estimated from the difference between the observed and predicted number of events in the first few bins ($N_{missed} = N_{expected} - N_{observed}$). $N_{expected}$ was approximated from the rate constant from a single exponential fit of the existing data by integrating $\frac{1}{k_{obs}} * e^{-k_{obs}t}$ from t = 0 ms to 40 ms, where k_{obs} is the rate constant from the single exponential fit of the existing data. As the time constant for a single exponential process is equal to the average dwell time (τ = <dwell time>), the correct rate constant, $k_{corrected}$, can be estimated from the proportion, $\frac{k_{obs}}{N_{obs}} = \frac{k_{corrected}}{N_{obs} + N_{missed}}$.[S23] The increase in k_{undock} estimated in this way was small (≤30%).

When undercounting of docked events was observed, a small slow phase, composed of very long, statistically unlikely events, appears in the undocked time integral plot (<5%, $k_{dock}^{(2)}$ < 1 s^{-1}) (Fig 3*c*). Such a slow phase of docking may result from more severe undercounting of undocked events in particular molecules, such as those with lower than average signal-to-noise. Because of the variable but small amplitude of the second phase in undocked time plots, such slow second phases were neglected.

Under conditions in which the rate constant for docking was greater than ~4 s^{-1}, an analogous correction for missing undocked events was applied to the rate constant for docking. Corrections to the rate constants for docking due to undercounting of undocking events increased the rate constant by <30%.

Calculation of K_{dock}. The reported equilibrium constants for docking were calculated from the ratio of the total time spent in the docked state and the total time spent in the undocked state [$K_{dock,total}$ = (time docked)/(time undocked)]. 'Total time' includes times at the beginnings and endings of traces that are not complete events because they are truncated by the start of observing a molecule, photobleaching, or the end of the observation time. In contrast, K_{dock} calculated from the ratio of rate constants ($K_{dock,kinetc} = k_{dock}/k_{undock}$), uses only complete events which provide information about the probability of changing states over time. Compared with $K_{dock,kinetic}$, $K_{dock,total}$ includes more data, is relatively insensitive to biases that influence rate constants, and, thus, is more accurate. Specifically, $K_{dock,total}$ is insensitive to the misidentification of short undocked events due to blinking as they contribute only a small amount to the total time spent in the undocked state. Further, because the equilibrium constant calculated from total times includes times that were interrupted by the beginning and end of a trace, $K_{dock,total}$ is also less sensitive to biases in the data due to short observation time relative to the sum of the time constants of a process. When the observed rate constants are corrected for systematic biases as described above, $K_{dock,total}$ and $K_{dock,kinetic}$ converge within error in nearly all cases. The largest difference observed between $K_{dock,total}$ and $K_{dock,kinetic}$, is in the 5 M urea data set for which the $K_{dock,total}$ is 0.10 ± 0.03 and $K_{dock,kinetic}$ is 0.3 ± 0.1. A possible origin of 2- to 4-fold lower $K_{dock,total}$ is heterogeneity in the ribozyme population at high urea (unpublished results). Our conclusions are unaffected by this data point.

Error Estimates. Reported errors are two standard deviations based on Poisson statistics. Two standard deviations are reported because no correction is made for systematic or experimental errors, which are more difficult to estimate, but appear to be relatively small

(<2-fold for [0.01 < K_{dock} < 100], see also Reproducubility, below). Errors are proportional to $\frac{1}{\sqrt{N}}$, where N is the number of observations. For processes described by a single exponential, the error is $\frac{\tau}{\sqrt{N}}$, where $\tau = \frac{1}{k}$. Errors of rate constants from double exponential fits were estimated using the number of events that contribute to each phase. This may be an underestimate, as the interdepence of the two phases increases the error of the fit. On the other hand, maximum likelihood analysis[S23] in which the first few time bins are excluded from data of wt ribozyme (L-21), d24, and d(-1) + G gives the same rate constants and errors as reported for the rate constants for docking and undocking. These data sets were examined because they contained a relatively large fraction of blinking events which might have significantly increased the errors associated with the reported rate constants.

The certainty associated with K_{dock} is related to the number of observed transitions between the docked and undocked states. The number of events that contributed to K_{dock} was estimated from the number of events from which each rate constants was determined, so that, $s(K_{dock})$, the error on K_{dock}, is equal to $K_{dock} \times \sqrt{\left(\frac{1}{N_{k_{dock}}}\right)^2 + \left(\frac{1}{N_{k_{undock}}}\right)^2}$, where $N_{k_{dock}}$ and $N_{k_{undock}}$ represent the number of undocked and docked events observed, respectively. Errors in $\Delta\Delta G$ and Φ-values are the probable errors (as opposed to maximal) based on the uncertainty of their components.[S24] These are calculated by adding in quadrature the partial derivative of the value being calculated, with respect to the component, multiplied by the error of the component. For example, s_{Φ}, the probable error on Φ is given by,

$$s_{\Phi} = \sqrt{\left[\left(\frac{\delta\Phi}{\delta K}\right)_k dK\right]^2 + \left[\left(\frac{\delta\Phi}{\delta k}\right)_K dk\right]^2} = \Phi\sqrt{\left(\frac{dK}{K}\right)^2 + \left(\frac{dk}{k}\right)^2}$$, where dK and dk are the errors on K and k.

Errors on the slopes of urea versus ln K or k plots were determined by least squares fits of constants calculated from the extremes of the errors. For example, for K_{dock} which decreases with urea, the slope of a line through the largest K_{dock} values at low urea and through the smallest K_{dock} values at high urea was compared with the slope of the line through the fit values. This conservative method was used because the systematic errors in measurements are greater when the equilibrium for docking is far from one, and so the points at the extreme urea concentrations contribute inordinately to the errors. Reported errors for the thermodynamic and activation parameters for docking are twice the standard errors from non-linear least squares curve fits.

Reproducibility. All reported rate constants are based on ≥50 events and in most cases, >500 events (generally, when K_{dock} is between 3 and 0.3). Measurements of the effects of modifications to the P1 duplex and other perturbations were made on two to four separate days with up to seven determinations, with some exceptions. The exceptions, which were each measured once, are as follows: d23, d26, the IGS modifications made in the context of the extended ribozyme (L-16), and the double modifications. For the measurements of single modifications made only once, the effects on K_{dock} are similar to previously reported effects.[S3,S4] Each urea point was measured once, but on four different days and non-sequentially with respect to urea concentration. Temperature data were collected on three different days with overlapping ranges. The ribozymes d25, I22, and d24 were constructed

twice and each preparation was examined one or more times. When available, the reported rate and equilibrium constants for a given modification or perturbation are based on a compilation of dwell time data measured on different days into one large data set for plotting and fitting. For the temperature data, identical temperatures are treated separately.

The observed variability in K_{dock} and k_{undock} from day-to-day was within two standard deviations of statistical error except in one case, d(-1). For this complex, K_{dock} was measured four times, and twice was found to be 3-fold less than the value reported in Table 1A (and k_{undock} 3-fold greater). Previous studies have found no effect of d(–1) on tertiary interactions,[S25,S3,S4] supporting the higher equilibrium constant which is within error of that for wt (Table 1A). The modest variation does not qualitatively effect the results. Beyond experimental error or partial degradation of the ribozyme sample, we cannot account for origin of the variability for this complex.

The observed variability in k_{dock} from day-to-day was generally within two standard deviations by statistical error. For wt ribozyme, variability in k_{dock} was within three standard deviations of statistical error, corresponding to a 2-fold difference in k_{dock} on different days ($k_{dock}^{(2)} = 1.6 \pm 0.7$ to 3.8 ± 0.9 s^{-1}). The origin of this larger than expected variability may be due, at least in part, to blinking. The day-to-day variation in k_{dock} with wt is within the small differences observed for k_{dock} with different modifications. However, the trends observed in the variations in k_{dock} for the modifications suggest that the small differences may be real (see Discussion).

REFERENCES

S1. Knitt, D. S., Narlikar, G. J. & Herschlag, D. (1994). Dissection of the role of the conserved G•U pair in group I RNA self-splicing. *Biochemistry* **33**, 13864-13879.

S2. Narlikar, G. J. & Herschlag, D. (1998). Direct demonstration of the catalytic role of binding interactions in an enzymatic reaction. *Biochemistry* **37**, 9902-9911.

S3. Narlikar, G. J., Khosla, M., Usman, N. & Herschlag, D. (1997). Quantitating tertiary binding energies of 2' OH groups on the P1 duplex of the *Tetrahymena* ribozyme: intrinsic binding energy in an RNA enzyme. *Biochemistry* **36**, 2465-2477.

S4. Strobel, S. A. & Cech, T. R. (1993). Tertiary interactions with the internal guide sequence mediate docking of the P1 helix into the catalytic core of the *Tetrahymena* ribozyme. *Biochemistry* **32**, 13593-13604.

S5. Strobel, S. A. & Cech, T. R. (1995). Minor groove recognition of the conserved G•U pair at the *Tetrahymena* ribozyme reaction site. *Science* **267**, 675-679.

S6. McConnell, T. S. & Cech, T. R. (1995). A positive entropy change for guanosine binding and for the chemical step in the *Tetrahymena* ribozyme reaction. *Biochemistry* **34**, 4056-4067.

S7. Shan, S. O. & Herschlag, D. (1999). Probing the role of metal ions in RNA catalysis: kinetic and thermodynamic characterization of a metal ion interaction with the 2'-moiety of the guanosine nucleophile in the *Tetrahymena* group I ribozyme. *Biochemistry* **38**, 10958-10975.

S8. Bevilacqua, P. C., Johnson, K. A. & Turner, D. H. (1993). Cooperative and anticooperative binding to a ribozyme. *Proc. Natl. Acad. Sci. USA* **90**, 8357-8361.

S9. Narlikar, G. J., Bartley, L. E., Khosla, M. & Herschlag, D. (1999). Characterization of a local folding event of the *Tetrahymena* group I ribozyme: Effects of oligonucleotide substrate length, pH, and temperature on the two substrate binding steps. *Biochemistry* **38**, 14192-14204.

S10. Narlikar, G. J., Gopalakrishnan, V., McConnell, T. S., Usman, N. & Herschlag, D. (1995). Use of binding energy by an RNA enzyme for catalysis by positioning and substrate destabilization. *Proc. Natl. Acad. Sci. USA* **92**, 3668-3672.

S11. Russell, R. & Herschlag, D. (1999). New pathways in folding of the *Tetrahymena* group I RNA enzyme. *J. Mol. Biol.* **291**, 1155-1167. doi:10.1006/jmbi.1999.3026.

S12. Narlikar, G. J. & Herschlag, D. (1996). Isolation of a local tertiary folding transition in the context of a globally folded RNA. *Nat. Struct. Biol.* **3**, 701-710.

S13. Li, Y., Bevilacqua, P. C., Mathews, D. & Turner, D. H. (1995). Thermodynamic and activation parameters for binding of a pyrene-labeled substrate by the *Tetrahymena* ribozyme: docking is not diffusion-controlled and is driven by a favorable entropy change. *Biochemistry* **34**, 14394-14399.

S14. Scaringe, S. A., Wincott, F. E. & Caruthers, M. H. (1998). Novel RNA synthesis method using 5'-O-silyl-2'-O-orthoester protecting groups. *J. Am. Chem. Soc.* **120**, 11820-11821.

S15. Engelhardt, M. A., Doherty, E. A., Knitt, D. S., Doudna, J. A. & Herschlag, D. (2000). The P5abc peripheral element facilitates preorganization of the *Tetrahymena* group I ribozyme for catalysis. *Biochemistry* **39**, 2639-2651.

S16. Zhuang, X., Bartley, L. E., Babcock, H. P., Russell, R., Ha, T., Herschlag, D. & Chu, S. (2000). A single molecule study of RNA catalysis and folding. *Science* **288**, 2048-2051.

S17. Moore, M. J. & Query, C. C. (2000). Joining of RNAs by splinted ligation. *Methods in Enzymol.* **317**, 109-123.

S18. Ha, T., Zhuang, X. W., Kim, H. D., Orr, J. W., Williamson, J. R. & Chu, S. (1999). Ligand-induced conformational changes observed in single RNA molecules. *Proc. Natl. Acad. Sci. USA* **96**, 9077-9082.

S19. Zhuang, X., Kim, H., Pereira, M. J., Babcock, H. P., Walter, N. G. & Chu, S. (2002). Correlating structural dynamics and function in single ribozyme molecules. *Science* **296**, 1473-1476.

S20. Kim, H. D., Nienhaus, G. U., Ha, T., Orr, J. W., Williamson, J. R. & Chu, S. (2002). Mg^{2+}-dependent conformational change of RNA studied by fluorescence correlation and FRET on immobilized single molecules. *Proc. Natl. Acad. Sci. USA* **99**, 4284-4289.

S21. Bevilacqua, P. C., Kierzek, R., Johnson, K. A. & Turner, D. H. (1992). Dynamics of ribozyme binding of substrate revealed by fluorescence-detected stopped-flow methods. *Science* **258**, 1355-1358.

S22. Bevilacqua, P. C., Li, Y. & Turner, D. H. (1994). Fluorescence-detected stopped flow with a pyrene labeled substrate reveals that guanosine facilitates docking of the 5' cleavage site into a high free energy binding mode in the *Tetrahymena* ribozyme. *Biochemistry* **33**, 11340-11348.

S23. Tamhane, A. C. & Dunlap, D. D. (2000). *Statistics and Data Analysis: From Elememtary to Intermediate*, Prentice Hall, Upper Saddle River, NJ.

S24. Sime, R. J. (1990). *Physical Chemistry: Methods, Techniques, and Experiments*, Saunders College Publisher, Philadelphia.

S25. Bevilacqua, P. C. & Turner, D. H. (1991). Comparison of binding of mixed ribose-deoxyribose analogues of CUCU to a ribozyme and to GGAGAA by equilibrium dialysis: evidence for ribozyme specific interactions with 2' OH groups. *Biochemistry* **30**, 10632-10640.

SUPPLEMENTARY FIGURE

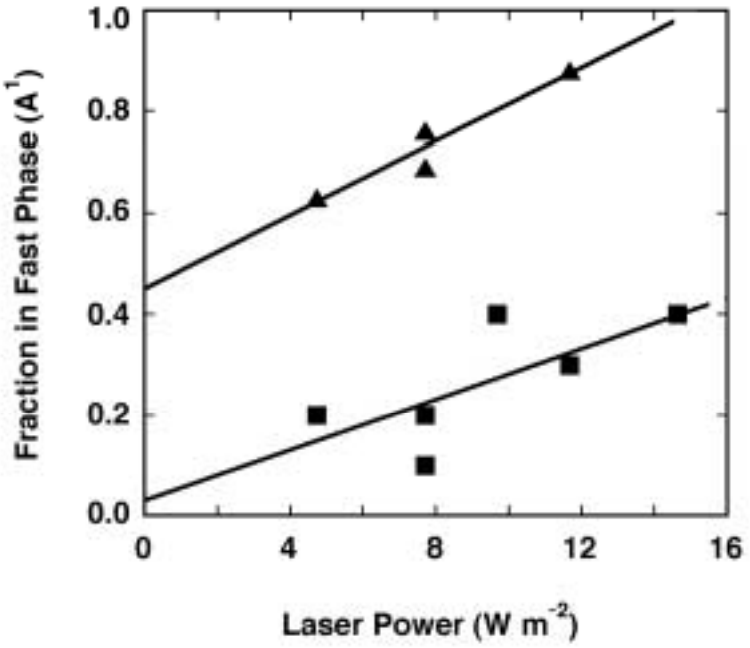

Fig S1. Dependence of the fraction in the fast phase in undocked dwell time plots for wt ribozyme (L-21) on the laser power (in Watts per meter^2) used to excite the sample. As in Figure 3*a* and 3*b*, undocked dwell time data for wt ribozyme were best fit with a double exponential equation (Eq S2), in which the amplitude of the faster phase is described by $A^{(1)}$. Time traces were analyzed with FRET criteria only, unscreened (▲),[§] and/or with FRET criteria and secondary screening criteria, screened (■),[§] as described in the Supplementary Materials and Methods. The linear fit of the unscreened data (▲) gives a slope of 0.036 W^{-1} m^2, with a y-intercept of 0.45 and a correlation coefficient (R) of 0.96 ($p < 0.03$). The linear fit of the screened data (■) gives a slope of 0.025 W^{-1} m^2, with a y-intercept of 0.03 and a correlation coefficient (R) of 0.72 ($p < 0.1$).